Multiferroicity in polarized single-phase $Bi_{0.875}Sm_{0.125}FeO_3$ ceramics

G. L. Yuan and Siu Wing Or[a)]
Department of Applied Physics, The Hong Kong Polytechnic University, Hung Hom, Kowloon, Hong Kong

(Received 10 December 2005; accepted 25 May 2006; published online 27 July 2006)

Single-phase $Bi_{0.875}Sm_{0.125}FeO_3$ ceramics were prepared, and their crystal structure and multiferroic properties were studied. The triclinic structure with $P1$ space group was confirmed in the ceramics by refining the x-ray diffraction data. Large piezoelectric d_{33} coefficient of 29 pC/N, together with high remnant polarization of 15.09 $\mu C/cm^2$, was measured at room temperature, suggesting the existence of long-range ferroelectric order on a macroscopic scale. The observed small remnant magnetization of 0.071 emu/g at room temperature as a result of the collapse of the space-modulated spin structure indicated the presence of long-range canted antiferromagnetic order on a macroscopic scale. The coexistence of the long-range ferroelectric and canted antiferromagnetic orders allowed the magnetoelectric effect below the antiferromagnetic Néel temperature of 265 °C near which magnetoelectric coupling was obvious. © *2006 American Institute of Physics*. [DOI: 10.1063/1.2220642]

I. INTRODUCTION

Multiferroic materials show both (anti)ferroelectric order and (anti)ferromagnetic order in the same phase. Thus they are prime candidates for displaying magnetoelectric (ME) effect defined as an induction of magnetization by means of an electric field or an induction of polarization by means of a magnetic field.[1] As an interesting candidate of multiferroic materials, single-phase $BiFeO_3$ possesses a high ferroelectric Curie temperature ($T_{C\text{-}FE}$) of ~830 °C and a high antiferromagnetic Néel temperature ($T_{N\text{-}AFM}$) of ~370 °C. These bring hope to community that ME effect may be observed at room temperature.[1–4] In fact, single-phase bulk $BiFeO_3$ exhibits a rhombohedral structure with space group $R3c$, where all ions along the $(111)_c$ direction are displaced relative to the ideal centrosymmetric positions and the oxygen octahedrons surrounding the transition-metal cations rotate alternately clockwise and counterclockwise about this $(111)_c$ direction.[5] Besides, it has canted G-type antiferromagnetic order combined with space-modulated spin structure on a long wavelength of 620 Å. However, the possible nonzero remnant magnetization (M_r) permitted by the canted G-type antiferromagnetic order is cancelled by the space-modulated spin structure on the 620 Å wavelength,[5–7] constraining the release and measurements of potential ME effect in the ceramic.[1]

In practice, two preconditions are required to enable potential ME effect in single-phase $BiFeO_3$ and its modified compositions. Precondition (1) states that samples should exhibit low-leakage ferroelectric behavior with reasonably large piezoelectric properties or, in general, long-range ferroelectric order.[1] Precondition (2) states that samples should display large M_r (or at least nonzero M_r) or, in general, long-range ferromagnetic order (or at least long-range canted antiferromagnetic order).[1] To meet precondition (1), single-phase samples with sufficiently low leakage current density (i.e., <30 mA/m^2 at 150 kV/cm field) have to be prepared to avoid dielectric breakdown during poling. Unfortunately, this is not the usual case in bulk $BiFeO_3$ and its modified compositions since there exist considerable amounts of charged defects governed by Fe^{2+} ion, oxygen vacancy (V_O^{2+}), and/or bismuth vacancy (V_{Bi}^{3-}) in the bulk samples, due to the transformation of Fe^{3+} ion to Fe^{2+} ion and/or volatilization of Bi^{3+} ion, according to the following reaction mechanisms:[8,9]

$$2Fe^{3+} + O^{2-} \Rightarrow 2Fe^{2+} + 0.5O_2(\text{volatization}) + V_O^{2+}, \quad (1)$$

$$2Bi^{3+} + 3O^{2-} \Rightarrow Bi_2O_3(\text{volatization}) + 2V_{Bi}^{3-} + 3V_O^{2+}. \quad (2)$$

Importantly, the presence of V_O^{2+} vacancy as stated in Eqs. (1) and (2) has the predominant effect on the reduction of the electrical resistivity of the bulk samples, giving rise to high leakage currents in the samples.[8,9] To meet precondition (2), either the canted antiferromagnetic order or the space-modulated spin structure has to be destroyed. However, effective ways to destroy canted antiferromagnetic order without weakening ferroelectric order in multiferroic materials have not yet been found. Although it is possible to collapse the space-modulated spin structure using a superhigh magnetic field of >10 T,[5] the most convenient and economical way is to modify the crystal structure of $BiFeO_3$ by A-site substitution (e.g., $Bi_{1-x}A_xFeO_3$, A=La, Sm, etc.).[6,7] Recently, it has been shown that the space-modulated spin structure of $BiFeO_3$ can be collapsed by the A-site La substitution, resulting in a uniform canted antiferromagnetic order in the $Bi_{1-x}La_xFeO_3$ system.[6,7]

Compared with La^{3+} ion (radius=1.032 Å), Sm^{3+} ion (radius=0.958 Å) possesses a much smaller radius. This suggests that the effect of A-site substitution may further be enhanced if Sm^{3+} ion is used in substitution for Bi^{3+} ion (radius=1.030 Å) in the ordinary $BiFeO_3$ composition. In $Bi_{1-x}Sm_xFeO_3$ system, M_r may be enhanced by increasing the A-site Sm substitution, yet too much substitution may

[a)]Author to whom correspondence should be addressed; electronic mail: apswor@polyu.edu.hk

weaken the effect of ferroelectricity. Moreover, it is of great interest to know whether both the space-modulated spin structure can be collapsed by the *A*-site Sm substitution and $T_{\text{N-AFM}}$ can be decreased towards room temperature (since ME coupling is much larger at temperatures slightly below $T_{\text{N-AFM}}$). In this paper, we aim to prepare single-phase multiferroic $Bi_{0.875}Sm_{0.125}FeO_3$ samples and investigate their structural, ferroelectric, piezoelectric, canted antiferromagnetic, and magnetoelectric properties. Single-phase multiferroic $BiFeO_3$ samples are also prepared and characterized for comparison. The specific composition $Bi_{0.875}Sm_{0.125}FeO_3$ ($x=0.125$) is chosen because this composition satisfies preconditions (1) and (2) for the maximization of both remnant polarization (P_r) and M_r.[1]

II. EXPERIMENTAL DETAILS

A rapid liquid-phase sintering method with a high heating rate of 100 °C/s was applied to prepare single-phase $Bi_{0.875}Sm_{0.125}FeO_3$ and $BiFeO_3$ ceramics.[8–10] High-purity (>99%) oxide powders were weighted according to the nominal compositions of $Bi_{0.875}Sm_{0.125}FeO_3$ and $BiFeO_3$. Each type of powder was finely milled into sizes of <1 μm. After drying, the powders were mixed thoroughly with water and pressed uniaxially into disks of 3 mm diameter and 1 mm thickness. The disk samples were dehydrated at 150 °C for 10 h in a vacuum chamber before being sintered at a relatively high temperature of 855 °C for a short time of 20 min. All the preparation procedures were optimized in terms of single phase and low-leakage current density so as to meet precondition (1). Further details about the sample preparation can be found elsewhere.[8–10]

The crystal structure of the sintered samples was examined by an x-ray diffractometer (Brucker D8 Advance System) with a 2θ step size of 0.02° and at a scan rate of one step every 4 s. Simulation of crystal structure based on the measured x-ray diffraction (XRD) data was carried out using a Rietveld structure refinement software (FULLPROF 2000). The samples were then thinned down to 0.4 mm thick, and silver paste was applied on their two major surfaces as electrodes for subsequent measurements and poling. The relative dielectric constant (ε) and loss tangent ($\tan\delta$) of the samples were measured from 0.01 Hz to 1 MHz using a broadband dielectric spectrometer (Novocontrol Concept80). The polarization hysteresis (*P-E*) loop at 100 Hz was evaluated with a standard Sawyer-Tower circuit. The leakage current density versus electric field (*J-E*) curve was acquired using a multimeter (Keithley 2000) and a high-voltage amplifier (Trek P0621P). Based on the measured *P-E* loop and *J-E* curve, an optimal dc electric field of 150 kV/cm was applied to polarize the samples at room temperature in a silicon oil bath for 1 h. The piezoelectric d_{33} coefficient was measured at 60 Hz using a piezo-d_{33} meter (IAAS ZJ-30). The planer and thickness electromechanical coupling coefficients (k_p and k_t) and their associated mechanical quality factors ($Q_{\text{m,kp}}$ and $Q_{\text{m,kt}}$) were determined using an impedance analyzer (Agilent 4294A) according to the resonance method stated in the IEEE standard on piezoelectricity. The magnetization hysteresis (*M-H*) loop was evaluated using a superconducting quantum interference device (SQUID) (Quantum Design XL7d). The temperature dependence of both ε and $\tan\delta$ was obtained at 1 MHz using the impedance analyzer. The heat flow versus temperature curve was recorded using a differential thermal analyzer (DTA) (Netzsch STA449C Jupiter).

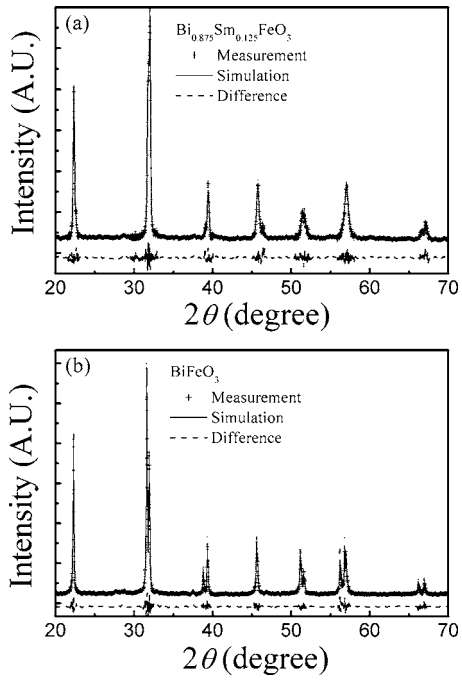

FIG. 1. Comparisons between the measured and simulated XRD patterns of (a) $Bi_{0.875}Sm_{0.125}FeO_3$ and (b) $BiFeO_3$ samples.

III. RESULTS AND DISCUSSION

Figure 1 shows the comparisons between the measured and simulated XRD patterns of $Bi_{0.875}Sm_{0.125}FeO_3$ [Fig. 1(a)] and $BiFeO_3$ [Fig. 1(b)] samples. From the measured XRD patterns (the + symbol), it is clear that $Bi_{0.875}Sm_{0.125}FeO_3$ and $BiFeO_3$ all have a single-phase perovskite structure with no trace of other impurity phases (e.g., Fe_2O_3, Bi_2O_3, $Bi_2Fe_4O_9$, etc.) within the uncertainty of XRD. Compared to $BiFeO_3$, some peaks of $Bi_{0.875}Sm_{0.125}FeO_3$ undergo a shift in 2θ and/or a combination of neighboring peaks, especially in the 2θ ranges of 31°–33° and 38.5°–40.5°. This indicates the existence of structural transformation between $Bi_{0.875}Sm_{0.125}FeO_3$ and $BiFeO_3$.

In order to further analyze such transformation, the measured XRD patterns of both $Bi_{0.875}Sm_{0.125}FeO_3$ and $BiFeO_3$ samples were used in Rietveld refinement of crystal structures based on a triclinic structure with $P1$ space group. In more detail, the crystal structure of $Bi_{0.875}Sm_{0.125}FeO_3$ was taken to be a triclinic structure with $P1$ space group, while the rhombohedral structure with $R3C$ space group that was previously reported in single-phase $BiFeO_3$ was considered as a special triclinic structure with $P1$ space group in the refinement process for ease of comparison of the refinement results.[10,11] As shown in Fig. 1, the simulated XRD patterns (the solid line) agree well with the measured XRD patterns, though they show slight variations (the dashed line) between each other. From the refined structural parameters tabulated in Table I, the generally small *R* values of Rietveld structure

TABLE I. The refined structural parameters of $Bi_{0.875}Sm_{0.125}FeO_3$ and $BiFeO_3$ samples based on the measured XRD patterns shown in Fig. 1 and according to a triclinic structure with $P1$ space group.

Material	Crystal structure	Lattice parameters	Atomic positions and volume	R values of Rietveld structure refinement
$Bi_{0.875}Sm_{0.125}FeO_3$	Triclinic structure	a=3.943 Å	Bi (0,0,0)	R_{wp}=7.19%
		b=3.957 Å	Fe (0.5198,0.5566,0.5011)	R_p=4.96%
		c=3.915 Å	O-1 (0.0960,0.5632,0.6754)	
		α=89.63°	O-2 (0.5091,−0.0937,0.4868)	
		β=89.82°	O-3 (0.6216,0.1345,−0.0524)	
		γ=89.72°	Volume=61.073 Å^3	
$BiFeO_3$	Rhombohedral structure	a=3.942 Å	Bi (0,0,0)	R_{wp}=6.36%
		b=3.942 Å	Fe (0.5967, 0.5045, 0.5724)	R_p=4.72%
		c=3.942 Å	O-1 (0.0404,0.5999,0.6513)	
		α=89.43°	O-2 (0.6114,0.0326,0.6116)	
		β=89.43°	O-3 (0.5638,0.6477,0.1456)	
		γ=89.43°	Volume=61.247 Å^3	

refinement (i.e., R_{wp}=7.19 and R_p=4.96 for $Bi_{0.875}Sm_{0.125}FeO_3$; R_{wp}=6.48 and R_p=4.76 for $BiFeO_3$) confirm that our $Bi_{0.875}Sm_{0.125}FeO_3$ samples have a single-phase triclinic structure with $P1$ space group, whereas our $BiFeO_3$ samples that show a single-phase rhombohedral structure with $R3c$ space group can be treated as a special triclinic structure with $P1$ space group. Nevertheless, the typical triclinic structure of $Bi_{0.875}Sm_{0.125}FeO_3$ (i.e., a =3.943 Å, b=3.957 Å, c=3.915 Å, α=89.63°, β=89.82°, and γ=89.72°) possesses comparatively larger a, b, α, β, and γ values, besides a relatively smaller c value, than the rhombohedral structure of $BiFeO_3$ (i.e., $a=b=c$=3.942 Å and $\alpha=\beta=\gamma$=89.43°) owing to the partial substitution of smaller Sm^{3+} ion for larger Bi^{3+} ion in $Bi_{0.875}Sm_{0.125}FeO_3$ samples.

Figure 2 illustrates the frequency (f) dependence of relative dielectric constant (ε) and loss tangent ($\tan\delta$) for $Bi_{0.875}Sm_{0.125}FeO_3$ and $BiFeO_3$ samples. Both $Bi_{0.875}Sm_{0.125}FeO_3$ and $BiFeO_3$ show decreasing tends in ε and $\tan\delta$ with increasing f from 0.01 Hz to 1 MHz. At sufficiently low f of <10 Hz, charged defects (V_O^{2+}, V_{Bi}^{3-}, and Fe^{2+}) are able to follow the applied electric field, resulting in increased ε and $\tan\delta$ values. At elevated f of >10 Hz, the weak dependence of ε and $\tan\delta$ on f, along with the generally low $\tan\delta$ values of <0.03, implies that electrons/domains rather than dipoles of the charged defects mainly contribute to the characteristics of ε and $\tan\delta$ above 10 Hz. $Bi_{0.875}Sm_{0.125}FeO_3$ samples possess larger ε and $\tan\delta$ in the whole f range of measurement when compared with the $BiFeO_3$ samples. This may be attributed to the formation of relatively stronger dipoles in the triclinic structure.

Figure 3 plots the polarization hysteresis (P-E) loops of $Bi_{0.875}Sm_{0.125}FeO_3$ samples measured at 100 Hz for three maximum electric fields (E_m) of 108, 150, and 167 kV/cm. The correspondingly measured remnant polarizations (P_r) are 0.52, 9.80, and 15.09 $\mu C/cm^2$, respectively. Although Bi^{3+} ion has been partially substituted by Sm^{3+} ion, the obvious ferroelectricity in our $Bi_{0.875}Sm_{0.125}FeO_3$ samples may be explained by what was found in $BiRO_3$ (R=Fe, Mn, Cr, etc.) systems that a lone s^2 pair of electrons of a Bi^{3+} ion may hybridize with an empty p orbital of a Bi^{3+} ion or an O^{2-} ion to form a localized lobe, giving rise to noncentrosymmetrically distorted structure and hence ferroelectricity.[1,12] It should be noted that our $Bi_{0.875}Sm_{0.125}FeO_3$ samples exhibit the largest maximum polarization (P_m) of 20.78 $\mu C/cm^2$, in addition to the largest P_r of 15.09 $\mu C/cm^2$, at the maximally allowed E_m of 167 kV/cm without being subjected to dielectric breakdown. Importantly, these P_m and P_r values are significantly larger than the largest reported P_m of 8.9 $\mu C/cm^2$ and P_r of 4 $\mu C/cm^2$ at the maximally allowed E_m of

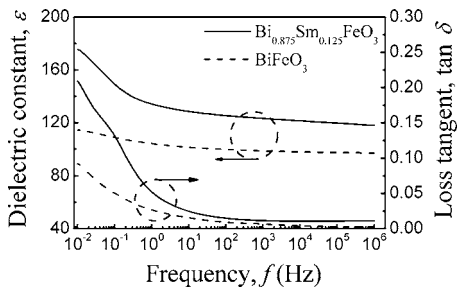

FIG. 2. Frequency (f) dependence of relative dielectric constant (ε) and loss tangent ($\tan\delta$) for $Bi_{0.875}Sm_{0.125}FeO_3$ and $BiFeO_3$ samples.

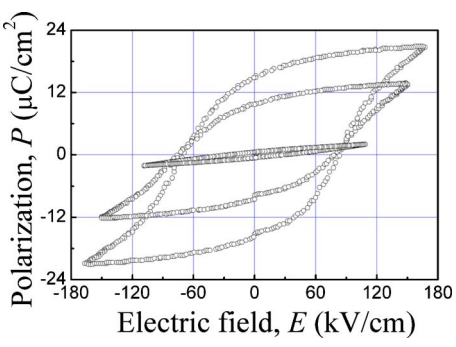

FIG. 3. Polarization hysteresis (P-E) loops of $Bi_{0.875}Sm_{0.125}FeO_3$ samples measured at 100 Hz for three maximum electric fields of 108, 150, and 167 kV/cm.

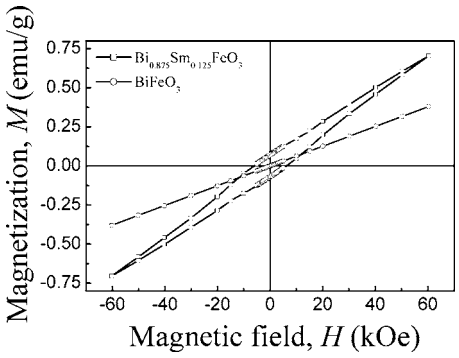

FIG. 4. Magnetization hysteresis (M-H) loops of $Bi_{0.875}Sm_{0.125}FeO_3$ and $BiFeO_3$ samples for the maximum magnetic field of 60 kOe.

100 kV/cm in single-phase bulk $BiFeO_3$.[10] In agreement with our $BiFeO_3$ samples, the P-E loop of $BiFeO_3$ may not technically saturate at its maximally allowed E_m (=100 kV/cm) due to the presence of much charged defects (and hence a larger leakage current density) in $BiFeO_3$ samples.[13–15] This also implies that the increased E_m in our $Bi_{0.875}Sm_{0.125}FeO_3$ samples should be one of the main factors in the increased P_m and P_r. In addition, the use of the optimized preparation procedures described in Sec. II is beneficial to the suppression of the charged defects.[8]

To enable measurements of the piezoelectric properties, $Bi_{0.875}Sm_{0.125}FeO_3$ samples were polarized using an optimal dc electric field of 150 kV/cm at room temperature for an hour. The *in situ* measurement of the electric field dependence of leakage current density (J-E) revealed a gradual increase in J with increasing E, and a sufficiently low J of $\sim$28 mA/m^2 at E=150 kA/m was achieved in the polarization process. This measured J should be the real J rather than the contribution of domain switching. Also, it is generally considered to be small enough to enable an effective polarization of multiferroic ceramics.[9] Thereafter, some important piezoelectric coefficients were measured according to the procedures mentioned in Sec. II. These piezoelectric coefficients include piezoelectric d_{33} coefficient (=29.2 pC/N), planer electromechanical coupling coefficient (k_p=0.154), thickness electromechanical coupling coefficient (k_t=0.283), planer mechanical quality factor ($Q_{m,kp}$=251.9), and thickness mechanical quality factor ($Q_{m,kt}$=42.4). The success in polarizing the samples and measuring the favorable ferroelectric behavior and piezoelectric properties suggest that the required long-range ferroelectric order as described by precondition (1) has been achieved in our $Bi_{0.875}Sm_{0.125}FeO_3$ samples.[1]

Figure 4 shows the magnetization hysteresis (M-H) loops of $Bi_{0.875}Sm_{0.125}FeO_3$ and $BiFeO_3$ samples for the maximum magnetic field (H_m) of 60 kOe. It is obvious that a small but nonzero remnant magnetization (M_r) of 0.071 emu/g, together with a coercive field (H_c) of 6.12 kOe, is achieved in $Bi_{0.875}Sm_{0.125}FeO_3$ samples, reflecting the presence of the required long-range canted antiferromagnetic order as stated in precondition (2). By contrast, both M_r and H_c vanish in $BiFeO_3$ samples because of the cancellation effect of the space-modulated spin structure.[5–7] Nevertheless, it is necessary to clarify whether the observed

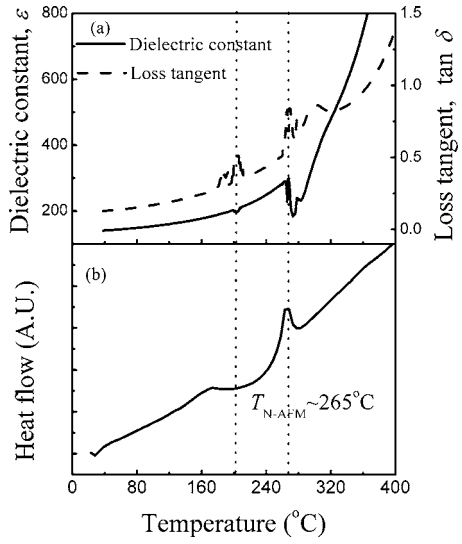

FIG. 5. (a) Temperature dependence of relative dielectric constant (ε) and loss tangent (tan δ) at 1 MHz for $Bi_{0.875}Sm_{0.125}FeO_3$ samples and (b) heat flow vs temperature curve for the samples.

M_r (and H_c) in $Bi_{0.875}Sm_{0.125}FeO_3$ truly originates from the collapse of the space-modulated spin structure or it is caused by other factors such as the presence of Fe_2O_3 and/or $Bi_2Fe_4O_9$ impurity phases, the contribution of charged defects, and the change from canted antiferromagnetic order to ferromagnetic order. The clarification is as follows: First, our $Bi_{0.875}Sm_{0.125}FeO_3$ samples have a larger H_c (=6.12 kOe) than ferromagnetic Fe_2O_3 impurity ($<$100 Oe); it is impossible that the observed M_r is a result of the small amount of Fe_2O_3 impurity left in the samples. Second, as the Curie temperature of $Bi_2Fe_4O_9$ impurity is much lower than the room temperature, $Bi_2Fe_4O_9$ should have null effect on M_r at room temperature.[16] Third, since reduced charged defects have been evidenced in our $Bi_{0.875}Sm_{0.125}FeO_3$ samples by the significantly large P_m (=20.78 μC/cm^2) and P_r (=15.09 μC/cm^2) for the maximally allowed E_m (=167 kV/m) and the sufficiently low J ($\sim$28 mA/m^2) even at a high E (=150 kV/cm), these limited charged defects may not be able to produce an influential effect on crystal structure and M_r. Finally, the change from canted antiferromagnetic order to ferromagnetic order can also be excluded because such change should accompany a large M_r. Therefore, the observed M_r in our $Bi_{0.875}Sm_{0.125}FeO_3$ samples is likely due to the collapse of the space-modulated spin structure. Indeed, the transformation from the rhombohedral structure with space group $R3c$ in $BiFeO_3$ to typical triclinic structure with $P1$ space group in $Bi_{0.875}Sm_{0.125}FeO_3$ leads to the collapse of the space-modulated spin structure.

Figure 5(a) shows the temperature dependence of ε and tan δ at 1 MHz of $Bi_{0.875}Sm_{0.125}FeO_3$ samples. It is found that dielectric anomalies take place at $\sim$265 and $\sim$202 °C. Since ferroelectric order and canted antiferromagnetic order have been confirmed in the samples at room temperature, these dielectric anomalies may result from paraelectric-ferroelectric (PE-FE) transition and/or magnetoelectric coupling. To obtain an insight into these anomalies, the heat flow versus temperature curve of the samples is also plotted in Fig. 5(b), in which two combined endothermic peaks are

observed at ~265 and ~790 °C (not shown). It is known that single-phase bulk $BiFeO_3$ samples not only have a dielectric anomaly and an endothermic peak at $T_{\text{N-AFM}}$ ~370 °C, but also possess an endothermic peak at $T_{\text{C-FE}}$ ~830 °C.[17] Considering these facts, it is believed that the endothermic peak of our $Bi_{0.875}Sm_{0.125}FeO_3$ at ~790 °C is caused by the PE-FE transition (i.e., $T_{\text{C-FE}}$ ~ 790 °C), while the dielectric anomaly and endothermic peak at ~265 °C originate from the magnetoelectric coupling (i.e., $T_{\text{N-AFM}}$ ~265 °C). With regard to the dielectric anomaly at ~202 °C, it may be due to magnetoelectric coupling when either the canting angle of canted antiferromagnetic order decreases to zero or the space-modulated spin structure disappears. Nevertheless, magnetoelectric coupling is observed below $T_{\text{N-AFM}}$ ~ 265 °C in our samples. This observed ME coupling and hence potential ME effect can be explained by the differentiation of free energy (F) in Eqs. (3) and (4) shown below:[1,18]

$$P_i(\mathbf{E},\mathbf{H}) = -\partial F/\partial E_i = P_i^S + \varepsilon_0\varepsilon_{ij}E_j + \alpha_{ij}H_j + (1/2)\beta_{ijk}H_jH_k + \gamma_{ijk}H_iH_j - \cdots, \quad (3)$$

$$M_i(\mathbf{E},\mathbf{H}) = -\partial F/\partial H_i = M_i^S + \mu_0\mu_{ij}H_j + \alpha_{ij}E_i + \beta_{ijk}E_iH_j + (1/2)\gamma_{ijk}E_jE_k - \cdots, \quad (4)$$

where $\mathbf{E}$, $\mathbf{H}$, P_i^S, M_i^s, α_{ij}, β_{ijk}, and γ_{ijk} are the electric field, magnetic field, spontaneous polarization along the i axis, spontaneous magnetization along the i axis, ME coefficient, higher-order ME coefficient according to $E_iH_jH_k$, and higher-order ME coefficient according to $H_iE_jE_k$, respectively. Disappearance of antiferromagnetic order can strongly impact ferroelectric order through α_{ij} and/or β_{ijk}/γ_{ijk} near $T_{\text{N-AFM}}$,[1] resulting in dielectric anomalies, i.e., ME coupling. When either the canting angle of canted antiferromagnetic order decreases to zero or the space-modulated spin structure disappears at temperatures below $T_{\text{N-AFM}}$, the vibration of antiferromagnetic order can also impact ferroelectric order through α_{ij} and/or β_{ijk}/γ_{ijk}, leading to dielectric anomalies. α_{ij} of single-phase bulk $BiFeO_3$ becomes zero in the absence of either long-range ferromagnetic order or long-range canted antiferromagnetic order, while both β_{ijk} and γ_{ijk} can still take effect.[1] Since obvious long-range ferromagnetic and canted antiferromagnetic orders have been verified in our $Bi_{0.875}Sm_{0.125}FeO_3$ samples at room temperature, α_{ij} should not be zero in our case. As ME coupling is commonly enhanced near $T_{\text{N-AFM}}$, the decrease in $T_{\text{N-AFM}}$ from ~370 °C of $BiFeO_3$ to ~265 °C of $Bi_{0.875}Sm_{0.125}FeO_3$ is favorable to enable large ME effect at room temperature.

IV. CONCLUSION

In conclusion, we have shown experimentally and simulationally that single-phase bulk $Bi_{0.875}Sm_{0.125}FeO_3$ multiferroic ceramics have a triclinic structure with $P1$ space group rather than the rhombohedral structure with $R3C$ space group in single-phase bulk $BiFeO_3$. Favorable piezoelectric properties and strong ferroelectric behavior have been measured in the ceramics at room temperature, confirming the presence of macroscopic long-range ferroelectric order. By collapsing the space-modulated spin structure, obvious canted antiferromagnetic behavior has been observed at room temperature, proving the existence of macroscopic long-range canted antiferromagnetic order. As a result, large ME coupling has been realized slightly below $T_{\text{N-AFM}}$ ~ 265 °C, allowing great prospect of measuring ME coefficients for device applications.

ACKNOWLEDGMENTS

This work was supported by the Research Grants Council of the HKSAR Government under Grant No. PolyU 5255/03E and the Center for Smart Materials of The Hong Kong Polytechnic University.

[1] M. Fiebig, J. Phys. D **38**, R123 (2005).
[2] J. Wang *et al.*, Science **299**, 1719 (2003).
[3] W. Eerenstein, F. D. Morrison, J. Dho, M. G. Blamire, J. F. Scott, and N. D. Mathur, Science **307**, 1203 (2005).
[4] K. Y. Yun, M. Noda, M. Okuyama, H. Saeki, H. Tabata, and K. Saito, J. Appl. Phys. **96**, 3399 (2004).
[5] B. Ruette, S. Zvyagin, A. P. Pyatakov, A. Bush, J. F. Li, V. I. Belotelov, A. K. Zvezdin, and D. Viehland, Phys. Rev. B **69**, 064114 (2004).
[6] A. V. Zalesskiĭ, A. A. Frolov, T. A. Khimich, and A. A. Bush, Phys. Solid State **45**, 141 (2003).
[7] Y. H. Lee, J. M. Wu, and C. H. Lai, Appl. Phys. Lett. **88**, 042903 (2006).
[8] G. L. Yuan and S. W. Or, Appl. Phys. Lett. **88**, 062905 (2006).
[9] G. L. Yuan, S. W. Or, Y. P. Wang, Z. G. Liu, and J. M. Liu, Solid State Commun. **138**, 76 (2006).
[10] Y. P. Wang, L. Zhou, M. F. Zhang, X. Y. Chen, J. M. Liu, and Z. G. Liu, Appl. Phys. Lett. **84**, 1731 (2004).
[11] A. K. Pradhan *et al.*, J. Appl. Phys. **97**, 093903 (2005).
[12] N. A. Hill and K. M. Rabe, Phys. Rev. B **59**, 8759 (1999).
[13] X. D. Qi, J. Dho, R. Tomov, M. G. Blamire, and J. L. MacManus-Driscoll, Appl. Phys. Lett. **86**, 062903 (2005).
[14] K. Y. Yun, D. Ricinschi, T. Kanashima, M. Noda, and M. Okuyama, Jpn. J. Appl. Phys., Part 2 **43**, L647 (2004).
[15] H. Béa *et al.*, Appl. Phys. Lett. **87**, 072508 (2005).
[16] V. A. Bokov, G. V. Novikov, V. A. Trukhtanov, and S. I. Yushchuk, Sov. Phys. Solid State **11**, 2324 (1970).
[17] V. R. Palkar, D. C. Kundaliya, S. K. Malik, and S. Bhattachary, Phys. Rev. B **69**, 212102 (2004).
[18] M. Fiebig, C. Degenhardt, and R. V. Pisarev, Phys. Rev. Lett. **88**, 027203 (2002).